Power Electronics and Reliability in Renewable Energy Systems

F. Blaabjerg, K. Ma, D. Zhou

Department of Energy Technology, Aalborg University
Pontopidanstraede 101, Aalborg East, 9220 Denmark
fbl@et.aau.dk, kema@et.aau.dk, zda@et.aau.dk

***Abstract*- Power Electronics are needed in almost all kind of renewable energy systems. It is used both for controlling the renewable source and also for interfacing to the load, which can be grid-connected or working in stand-alone mode. More and more efforts are put into making renewable energy systems better in terms of reliability in order to ensure a high availability of the power sources, in this case the knowledge of mission profile of a certain application is crucial for the reliability evaluation/design of power electronics. In this paper an overview on the power electronic circuits behind the most common converter configurations for wind turbine and photovoltaic is done. Next different aspects of improving the system reliability are mapped. Further on examples of how to control the chip temperature in different power electronic configurations as well as operation modes for wind power generation systems are given in order to reduce the temperature cycling.**

I. INTRODUCTION

In classical power systems, large power generation plants are located at adequate geographical places to produce most of the power, which is then transferred towards large consumption centers over long distance transmission lines. Now the power system is changing, as a large number of dispersed generation (DG) units, including both renewable and non-renewable sources such as wind turbines, wave generators, photovoltaic (PV) generators, small hydro, fuel cells and gas/steam powered Combined Heat and Power (CHP) stations, are being developed and installed all over the world [1]-[2]. A wide-spread use of renewable energy sources in distribution networks is seen. E.g. Denmark has a high power capacity penetration (> 30 %) of wind energy in major areas of the country and today 28 % of the whole electrical energy consumption is covered by wind energy. The main advantages of using renewable energy sources are the elimination of harmful emissions and the inexhaustible resources of the primary energy. However, the main disadvantage, apart from the higher costs is the uncontrollability as the renewable energy resources are completely weather-based. The availability of renewable energy sources has strong daily and seasonal patterns and the power demand by the consumers could have a very different characteristic. Therefore, it is difficult to operate a power system installed with only renewable generation units due to the characteristic differences and the high uncertainty in the availability of the renewable energy sources without any load control. This is further strengthened as no real large scale electrical energy storage systems exist.

The wind turbine technology is one of the most emerging renewable energy technologies [3]-[12]. It started in the 1980'es with a few tens of kW production power per unit to today with multi-MW size wind turbines that are being installed. It also means that wind power production in the beginning did not have any impact on the power system control but now due to their size they have to play an active part in the grid operation. The technology used in wind turbines was in the beginning based on a squirrel-cage induction generator connected directly to the grid. By that power pulsations in the wind are almost directly transferred to the electrical grid. Furthermore, there was no control of the active and reactive power except from some capacitor banks, which are important control parameters to regulate the frequency and the voltage in the grid system. As the power range of the turbines increases those control parameters become very important and power electronics [5] is introduced as an interface between the wind turbine and the grid. The power electronics is able to change the basic characteristic of the wind turbine from being an energy source to be an active electrical power source. The electrical technology used in wind turbine is not new. It has been discussed for several years but now the price pr. produced kWh is so low, that solutions with power electronics are very attractive .

The development of photovoltaic has also been progressive. Every year the price pr. produced kWh is decreasing by improving the PV-cells themselves as well as making the PV-inverters more efficient and reduce the prize. The PV-technology is working along a couple of technology lines – all need large investment to move from basic research to use in commercial large scale products. Power electronics is again the key to enable the photovoltaic technology to be connected to the grid system [13]-[19].

Both technologies are changing the grid to be much more uncontrolled and heterogeneous. Power system operators are developing new methods to control the grid – e.g. in a smart-grid structure where new demands to communication, control, safety, protection and so on are becoming defined [2].

The scope of this paper is first to give an overview on the developing trends and most commonly used power electronics for both wind and photovoltaic applications. Then different aspects of emerging reliability issues for power electronics in renewable energy systems are discussed and mapped. Finally, the thermal loading and improved control methods, which are closely related to the reliability of power electronics, are presented under various operation modes and configurations of wind power converter to illustrate the potentials.

II. Power Electronics for Wind Turbine and Photovoltaic Applications

As the quick development of technologies and various application requirements for renewable energies, there are many possible power converter configurations as well as circuit topologies in this field [20], [21]. Some of the most common and important converter configurations/circuits both for wind turbine and photovoltaic systems are presented below.

A. Configurations in wind power generation system.

In wind power generation system, the wind energy is converted to variable AC voltage/current by generators, therefore the AC-DC and DC-AC power conversion are dominant in this application to regulate the power.

As the state-of-the-art and most adopted solution for wind power generation, single-cell partial-scale power converter is used in conjunction with the Doubly-Fed Induction Generator (DFIG), as shown in Fig. 1 (a). The stator of DFIG is directly connected to the grid, while a partial-scale power converter is connected to the rotor to control the rotor frequency as well as current, with normal 30% rated power of generator. The smaller converter makes this concept attractive from an economical point of view. However, its main drawbacks are the use of slip-rings and the protection schemes/power controllability in the case of grid faults [23], [24], both of which decrease the availability to utilize the wind power source.

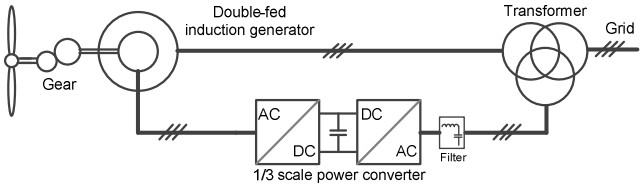

(a) Single-cell converter with partial-scale power.

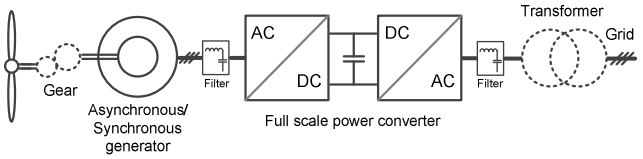

(b) Single-cell converter with full-scale power.

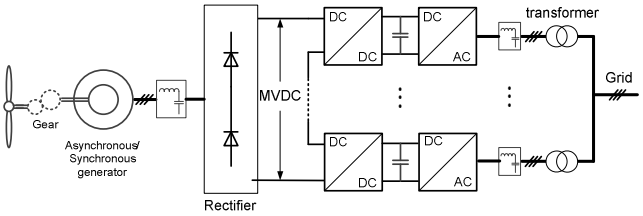

(c) Multi-cell converters with generator side series and grid side paralleled (Series-Parallel).

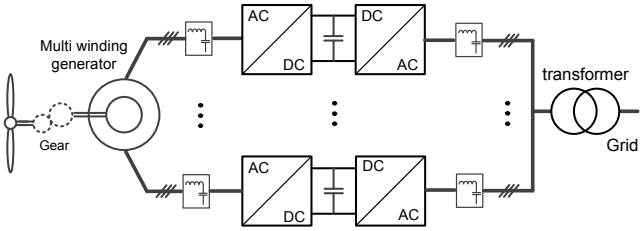

(d) Multi-cell converters with both generator side and grid side paralleled (Parallel-Parallel).

Fig. 1. Common configurations for wind power generation.

Another configuration that is becoming popular in the wind power application is shown in Fig. 1 (b). It introduces a single-cell full-scale power converter to achieve full power and full speed range control of the whole wind turbine system. In this solution the generator can be asynchronous generator, electrically excited synchronous generator (WRSG) or permanent magnet excited type (PMSG). The elimination of slip ring, more simple gearbox, as well as full power controllability during grid faults are the main advantages compared to the DFIG-based configuration. However as the fast growing power capacity of wind turbines, the more loading and expensive power electronics may raise some uncertainties for this solution to be further commercialized.

In the last few decades the power level of a single wind turbine was kept growing up in order to reduce the price pr. generated kWh. Nowadays most of the newly established wind turbines already range in multi-MW power level. In order to handle such fast growing high power, some multi-cell converter configurations (i.e. parallel/series connection of single-cell converters) are developed and widely adopted by the industry.

Fig. 1 (c) shows a multi-cell converter approach proposed by Semikron [24]: the single cell converters are connected in series on the generator side with a Medium Voltage (MV) DC bus, while the grid side converters are connected in parallel with separated transformers. The main advantage of this solution is that the standard low voltage power semiconductors can be used for higher power and voltage conversion. Also the redundancy features of the multi-cells increase the availability of this converter configuration.

Fig. 1 (d) shows another multi-cell solution adopted by Gamesa in the 4.5 MW wind turbines [25], which have single-cell converters paralleled both on the generator side and on the grid side. Siemens also introduce this kind of solution (paralleling the single cell converters) in some of their multi-MW wind turbines [26]. The standard and proven single-cell low voltage converters and redundant ability are the main advantages of this solution.

B. Topologies for wind power converter.

For the wind power application the power level is normally high in order to reduce the price pr. generated kWh, therefore three-phase converter topologies are dominant for wind turbine system.

Pulse Width Modulation-Voltage Source Converter with two-level output voltage (2L-PWM-VSC) is the most frequently used three-phase power converter topology in wind power systems. As the interface between the generator and power grid, two 2L-PWM-VSCs are usually configured

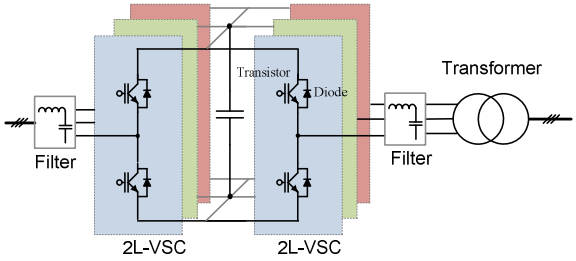

(b) Two-level back-to-back converter (2L-BTB)

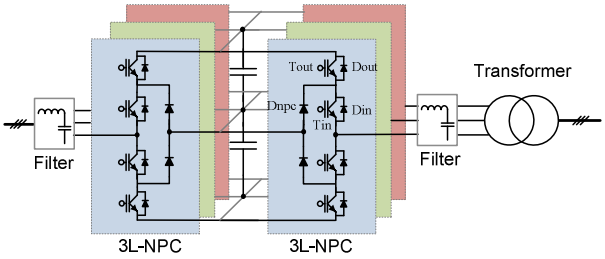

(b) Three-level Neutral-Point-Clamped back-to-back converter.(3L-BTB)

Fig. 2. Common power electronic topologies for wind power converter.

as a back-to-back structure (2L-BTB) with a transformer on the grid side, as shown in Fig. 2 (a). A technical advantage of the 2L-BTB solution is the relatively simple structure and few components, which contributes to a well-proven robust and reliable performance. However, as the increasing of power and voltage level, the 2L-BTB converter may suffer from larger switching losses, lower efficiency and higher *dv/dt* stresses to the generator and transformer [27].

The 2L-BTB topology is state of the art in DFIG based single cell converter configuration [6], [9], [12]. Some manufacturers are also using this topology for single-cell full-scale converter as well as multi-cell converter configurations.

Three-level Neutral Point diode Clamped topology is one of the most commercialized multi-level converter topologies on the market, the topology is shown in Fig. 2 (b), which is called 3L-NPC BTB for convenience. It achieves one more output voltage level and less *dv/dt* stress compared to the 2L-BTB topology, thus the filter size is smaller. The 3L-NPC BTB is also able to output the double voltage amplitude compared to the two-level topology by the switching devices of the same voltage rating. The mid-point voltage fluctuation of the DC-bus used to be a drawback of the 3L-NPC BTB. However, this problem has been extensively researched and is considered improved by the controlling of redundant switching status [28]. However, it is found that the loss distribution is unequal between the outer and inner switching devices in a switching arm, and this problem might lead to uneven lifetime of power switching devices and de-rated converter power capacity when it is practically designed [28]-[30].

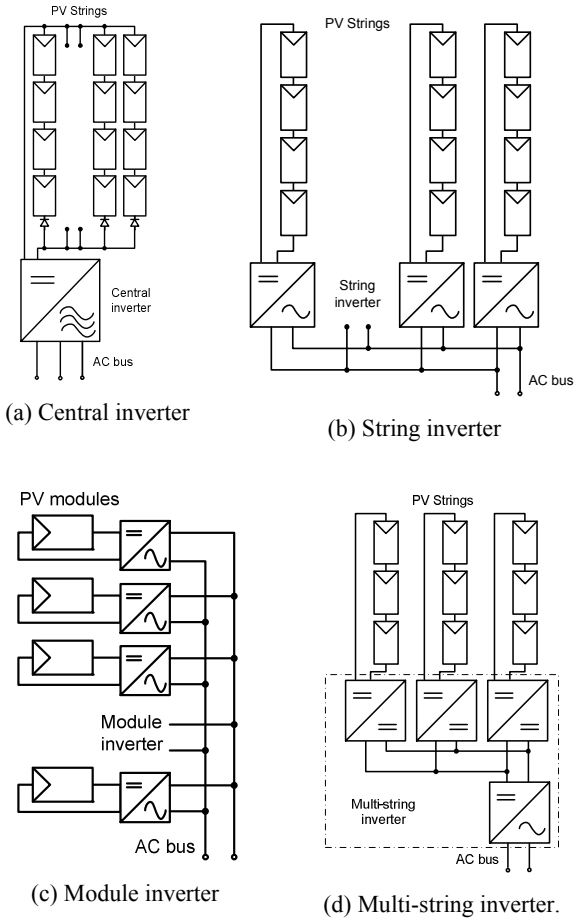

(a) Central inverter

(b) String inverter

(c) Module inverter

(d) Multi-string inverter.

Fig. 3. Common configurations for photovoltaic generation.

C. *Configurations in photovoltaic generation system.*

Different from the wind power system, the PV panels convert the solar energy to DC voltage/current, thereby the DC-DC and DC-AC conversions are dominant in the photovoltaic application [31]-[33]. A general classification of grid-connected PV inverters is as follows:

PV plants larger than 10 kWp arranged in parallel strings, are normally connected to one common central inverter (as shown in Fig. 3 (a)). However, the disadvantages are also significant: need for high-voltage DC cables between PV panels and inverter, power losses due to common maximum Power Point Tracking (MPPT), power loss due to module mismatch, losses in the string diodes, reliability of the whole system depends on one inverter only.

String inverters, as shown in Fig. 3 (b), were introduced into the European market in 1995. They are based on a modular concept, where PV strings, made up of series-connected solar panels, are connected to separate inverters. Then the string inverters are paralleled and connected to the grid. If the string voltage is high enough - no voltage boosting is necessary, thereby improving the efficiency. Fewer PV panels can also be used, but then a DC-DC converter or a line frequency transformer is needed for a boosting stage. The

advantages compared to the central inverter are: no losses in string diodes (no diodes needed), separate MPPTs for each string, better energy yield due to separate MPPTs, and lower price due to mass production.

Another converter configuration is module-based, in this structure a module is made up of a single solar panel connected to the grid through its own inverter, as shown in Fig. 3 (c). The advantage of this configuration is that there are no mismatch of losses, due to the fact that every single solar panel has its own inverter and MPPT, thus maximizing the power production. The power extraction is much better optimized than in the case of String inverters. One other advantage is the modular structure, which simplifies the modification of the whole system because of its "plug & play" characteristic. One disadvantage is the low overall efficiency due to the high-voltage amplification, and the price per watt is still higher than in the previous cases. But this can in the future maybe be overcome by mass production, leading to low manufacturing and retail costs [34].

Multi-String inverters have recently appeared on the PV market. They are an intermediate solution between String inverters and Module inverters. A Multi-String inverter, shown in Fig. 3 (d), combines the advantages of both String and Module inverters, by having many DC-DC converters with individual MPPTs, which feed energy into a common DC-AC inverter. In this way, no matter the nominal data, size, technology, orientation, inclination or weather conditions of the PV string, they can be connected to one common grid connected inverter [35], [36]. The Multi-String concept is a flexible solution, having a high overall efficiency of power extraction, due to the fact that each PV string is individually controlled.

D. Topologies for photovoltaic converter.

In the photovoltaic generation system the power level is normally much lower for each of the converter cell compared to the wind turbine application. As a result, single-phase converter topologies are dominant for the photovoltaic application. It is noted that the efficiency and ground current (which is determined by the common mode voltage) are two of the important considerations when evaluating PV converter topologies and their modulation methods. In the following different transformer-less PV-inverter technologies are focused as they can obtain the highest efficiency.

As shown in Fig. 4, the Boost + H-bridge topology introduce a boost DC-DC converter to first boost up and stabilize the voltage generated by PV strings, and then feed the power to a single phase H-bridge inverter, which is directly connected to the power grid. This topology has good adaption even for PV strings with lower output DC voltage. However the lower conversion efficiency is the main disadvantage.

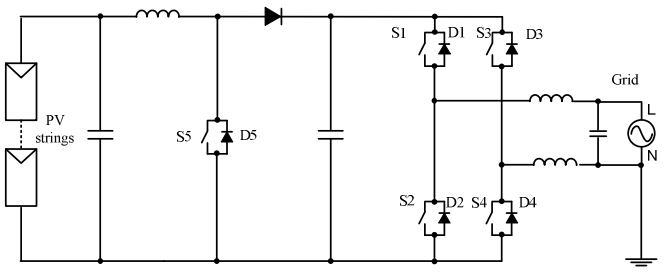

Fig. 4. Boost + H bridge topology for PV converter [13], [14].

The H-Bridge is a well-known topology and it is made up of two half bridges. To control the four switches in this topology several PWM techniques can be implemented. The simplest one is the bipolar PWM, which modulates switches T1-T4 (see Fig. 5) complementary to T2-T3, resulting in a two level output voltage level. The conversion efficiency is reduced due to the fact that during the free-wheeling period the grid current finds a path and flows back to the DC-link capacitor.

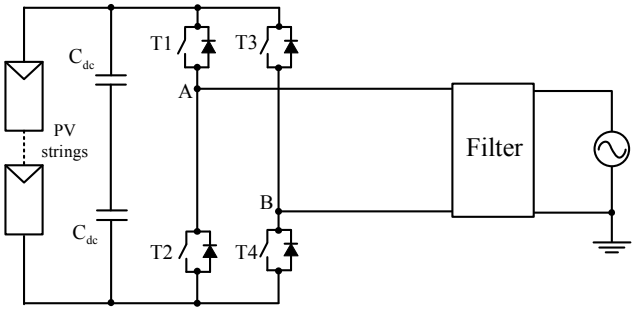

Fig. 5. H bridge topology for PV converter [13], [14].

The H5 bridge topology [37], used by SMA in many of their transformer-less inverters are using the same idea for the generation of the unipolar output voltage: disconnection of the PV array from the grid during the zero voltage state. The topology is shown in Fig. 6. The common-mode voltage behavior of the H5 topology is similar to the H-Bridge with bipolar PWM. The voltage to ground of the PV array terminals will only have a sinusoidal shape, while having the same high conversion efficiency as the H-Bridge with unipolar switching. Based on these results it can be stated that the H5 topology is suitable for transformer-less PV systems. Unipolar output voltage is achieved by disconnecting the PV array from the grid during the period of the zero voltage state, using a method called DC decoupling.

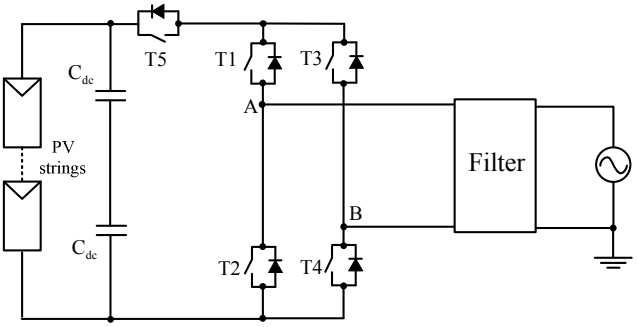

Fig. 6. H5 bridge topology for PV converter [37].

To keep high efficiency and keep all the advantages given by the unipolar PWM, but still have the common-mode behavior as in case of the bipolar PWM, the H-Bridge topology may be modified [38], the Highly Efficient and Reliable Inverter Concept (HERIC), as shown in Fig. 7. The modification includes two extra switches (T5-T6) each connected in series with a diode. There will be no high frequency fluctuations present at the DC terminals of the PV array. The common-mode behavior of the HERIC topology is similar to the H-Bridge with bipolar PWM. The voltage to ground of the PV array terminals will only have a sinusoidal shape, while having the same high conversion efficiency as the H-Bridge with unipolar switching. Based on these results, it can be stated that the HERIC topology is suitable for transformer-less PV systems.

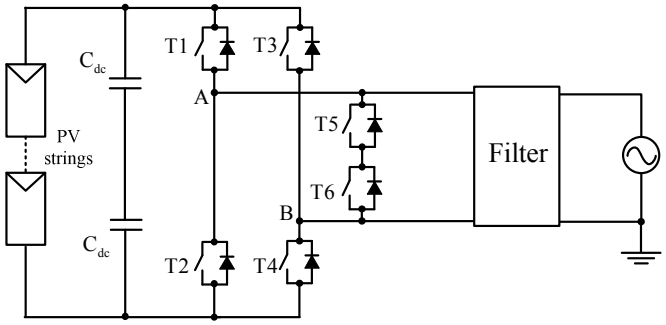

Fig. 7. HERIC topology for PV converter [38].

The single phase three-level Neutral Point Clamped (NPC) topology can also be used in the photovoltaic application. The connection of the neutral line of the middle point of the DC-link fixes the potential of the PV array to the grounded neutral [39]. Fig. 8 shows this topology. The NPC topology is suitable for transformer-less PV systems, since the voltage to ground is constant in the case of both terminals of the PV. The only drawback for the single-phase NPC topology is the higher DC-link voltage, which has more than twice the grid peak voltage and might reach voltages higher than the allowed maximum system voltage, therefore a boost stage may be needed before the inverter, which decreases the overall efficiency of the whole PV system.

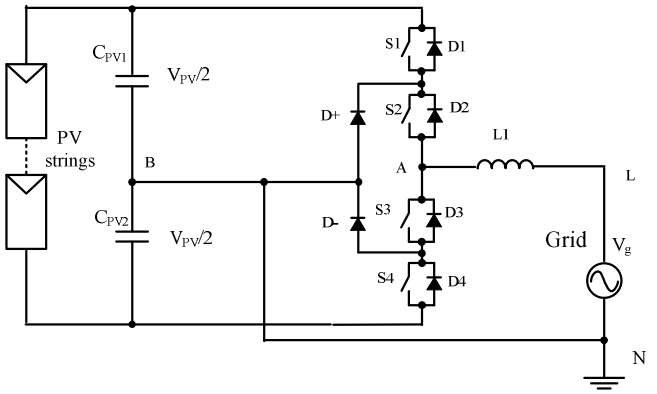

Fig. 8. 3L-NPC topology for PV converter [39].

.

III. Reliability Issues for Power Electronics in Wind Turbines

There are several significant trends for the development of wind power generation system in the last few decades: The penetration of wind power into the power grid is growing even expected to be 20% of the total electricity production at 2020 in Europe [40]. Meanwhile, the power capacity of a single wind turbine is increasing continuously in order to reduce the price pr. produced kWh. Moreover the location of wind farms is moving from onshore to offshore because of land limits and potentially richer wind energy resources. Consequently, due to much more significant impacts to the power grid and higher cost to repair after failures, the wind power generation system is required to be more reliable and able to withstand extreme grid/environment disturbances.

Unfortunately, former market feedbacks have shown that the larger wind turbines seem to be more easily having failures, as indicated in Fig. 9 [41], where the failure rates for different groups of wind turbines are indicated. When looking at the feedback failure rates and down time distribution in a wind turbine system, as shown in Fig. 10, the control and power converters tend to be easier to failure even though the generator and gearbox have the largest downtime (i.e. time needed for repair) [42].

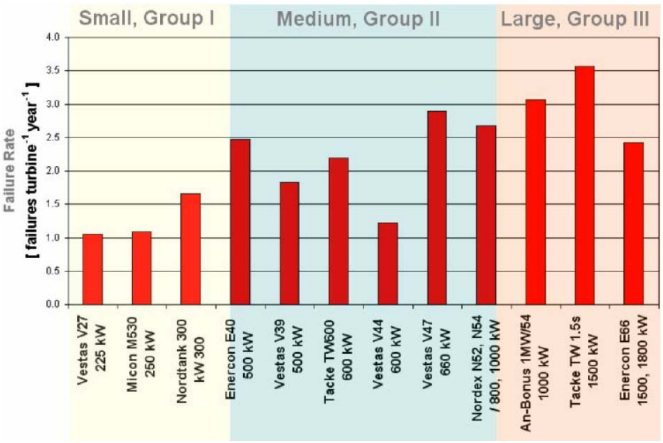

Fig. 9. Faulure rate of different wind turbines [41].

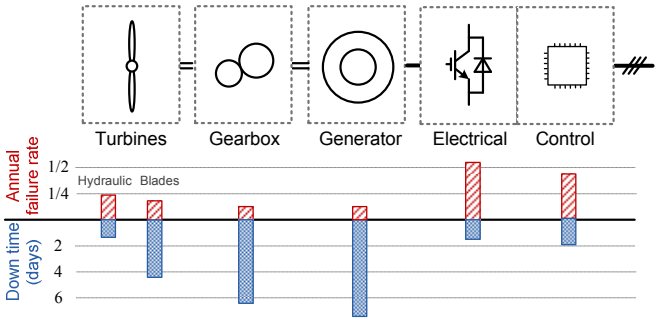

Fig. 10. Failure rate and down time for different parts of wind turbine [42].

As mentioned before, the power electronics is taking a much more important role in the utilization of renewable energy resources. Configuration for wind power generation is

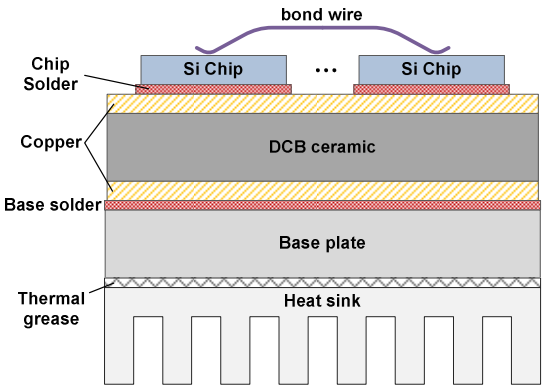

Fig. 11. Breakdown of different layers of materials in and IGBT module fastened on a heat sink [45].

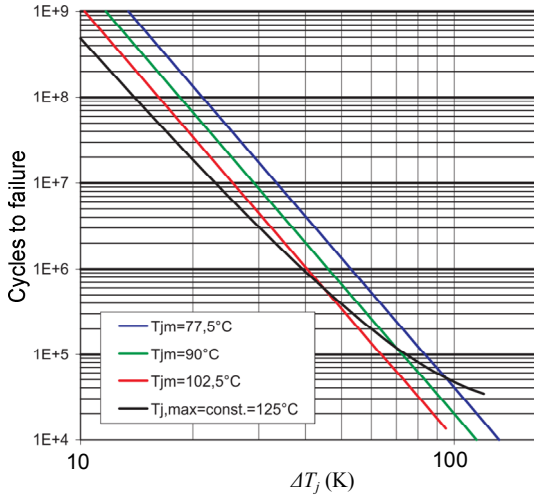

Fig. 12. Illustration of industrial standard cycles to failure vs. dTj of IGBT module by Semikron [46].

now being pushed from partial-scaled-converter system to full-scaled-converter system, which shown in Fig. 1 (b). This is mainly because full-scaled-converter system eliminates/simplifies the slip-ring and gearbox, enabling more robust mechanical part and full power controllability of the wind turbines. However, the introduced larger capacity power converters with more stressed and expensive power semiconductors may trade off the lifetime and cost of the electrical part. As a result, the reliability performance of the power electronics is a critical consideration and research topic for the modern wind power generation system.

The study of reliability in power electronics is moving from a statistically based approach that has been proven to be unsatisfactory in achieving higher safety levels in the automotive industry, to a physics-of-failure approach which involves the study of the root cause and the mechanism behind the failures (e.g. power devices but also other components) [43], [44].

Fig. 11 shows a breakdown of different layers of materials from chip to heat sink inside IGBT module [45], which is chosen as an example in this paper and this technology has been a popular power semiconductor device in the wind power application. It was found that the main driver for the power semiconductor failures is the thermal cycling of different layers of materials with mismatching expansion coefficients. The thermal cycling is a response to the converter loading changes as well as periodically commutation of power switching devices. The periodical losses generated from the silicon chips propagate through the thermal impedance between silicon chips and heat sink, causing temperature excursions at various frequencies/amplitudes on different layers of materials. Then the layers with different materials expand and compress until failure mechanisms are triggered. It has been widely accepted that the three dominant failure mechanisms for IGBT module are: the bond wire lift-off, solder joints cracking under the chip and solder joints cracking under the DCB ceramics, as indicated in Fig. 11 [46].

In order to relate the failure mechanisms and quantified reliability performance, some analytical models are developed to predict the lifetime (cycles to failure) of power semiconductors as a function of various details of thermal cycling information. Some of them are illustrated in the following [45]-[47]:

Coffin-Manson Model

$$N_f = \alpha \cdot (\Delta T_j)^{-n} \tag{1}$$

This is the simplest life time model which only takes into account the fluctuation of junction temperature ΔT_j. The α and n are constants which can be acquired experimentally.

Coffin-Manson-Arrhenius Model

$$N_f = \alpha \cdot (\Delta T_j)^{-n} \cdot e^{E_a/(k \cdot T_{jm})} \tag{2}$$

Besides ΔT_j this improved Coffin-Manson model also takes into account the mean junction temperature T_{jm}. K is the Boltzmann constant and E_a is activation energy parameter.

Norris-Landzberg Model

$$N_f = A \cdot f^{-n_2} \cdot (\Delta T_j)^{-n_1} \cdot e^{E_a/(k \cdot T_{jm})} \tag{3}$$

This model is based on (2) and additionally takes into

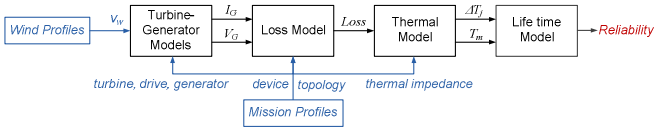

(b) Reliability prediction

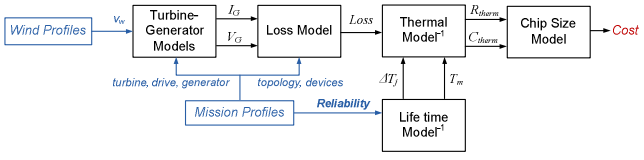

(b) Cost prediction

Fig. 13. Reliability-related evaluation methods for the wind power converter.

account the cycling frequency f of the junction temperature.

Bayerer Model

$$N_f = K \cdot (\Delta T_j)^{-\beta_1} \cdot e^{\beta_2/(T_{j\max}+273)} \cdot t_{on}^{\ \beta_3} \cdot I^{\beta_4} \cdot V^{\beta_5} \cdot D^{\beta_6} \quad (4)$$

The Bayerer model has a large number of parameters and it considers more detailed information during the power cycling tests and power module characteristics. Where T_{jmax} is the maximum junction temperature, t_{on} is the heating time, I is the applied DC current, D is the diameter of the bond wire, and V is the blocking voltage.

The parameters of these life time models are typically acquired based on experimental failure-accelerated test, where the power devices are running at different thermal cycling profiles until failures are observed. Afterwards the life time models are fitted to the test points. Fig. 12 shows an accelerated test example of IGBT modules by Semikron, in which a series of fitting curves are plotted to indicate the numbers of cycles to failure against different chip/junction temperature fluctuations ΔT_j under various mean junction temperatures T_{jm}.

With the quantified and physical life time models of power switching devices, there may be two ways to evaluate the converter system considering the reliability of power electronics, as shown in Fig. 13. The first way is to predict the life time of power semiconductors based on the existing converter design. The second way is to estimate the needed power devices based on a given reliability requirement. It can be seen that a clear mission profile, which includes the information of converter loading, converter configurations, as well as the loss and thermal behaviors of the chosen devices, are crucial important for the reliability evaluation process and results.

Besides the evaluation methods, some other potential works on the topic of power electronics reliability has been opened: e.g. further understanding and modeling of failure mechanisms/life time test of power semiconductors [48], [49], real time detection of the wear-out states of power devices [50], and thermal-oriented controls for power converters [51], etc.

IV. Thermal Loading and Control Methods for Wind Power Converters

Because the thermal performances of power semiconductors are closely related to the reliability as well as cost of the whole converter system, some examples regarding the thermal loading and methods to improve the thermal cycling in the wind power application are presented next.

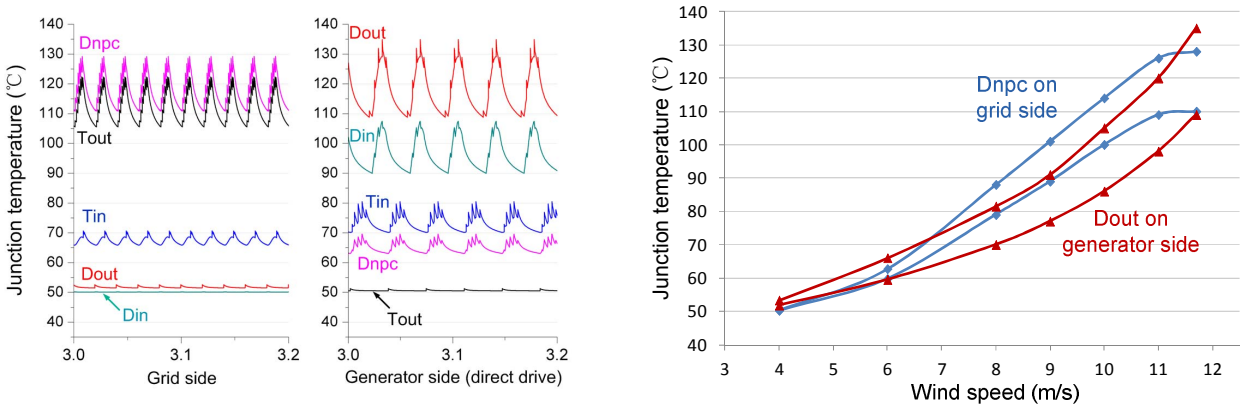

(a) Thermal distribution (b) Thermal profile of most stressed devices vs. wind speed

Fig. 14. Junction temperature profiles of 3L-NPC converter (10 MW, V_{ll} =3.3 kV, normal operation).

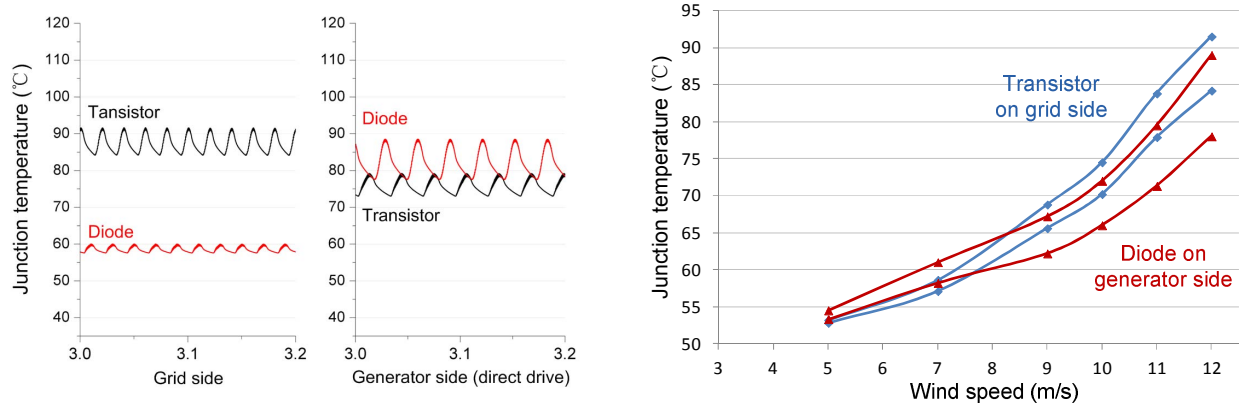

(a) Thermal distribution (b) Thermal profile of most stressed devices vs. wind speed

Fig. 15. Junction temperature profiles of 2L-NPC converter (2 MW, V_{ll} =690 V, normal operation).

A. Normal operation

In most of the life time models for power semiconductors, the junction temperature fluctuation ΔT_j and mean value T_{jm} are two of the most important indicators for the life time of power semiconductors, therefore it is important to extract the ΔT_j and T_{jm} information from a given converter design. According to the loss behavior and thermal impedance from the datasheets of chosen power devices, it is possible to estimate the junction temperature profile of power devices.

Table I. Parameters for the converters as study case.

Configurations	3L-NPC	3L-HB	5L-HB	2L
Rated power	10 MW			2 MW
Equivalent sw. freq.	Grid side: 800 Hz / Generator side : 275 Hz			2 kHz / 2 kHz
Fundamental freq.	Grid side: 50 Hz / Generator side : 27.5 Hz			50 Hz / 32 Hz
Rated output voltage	3.3 kV	3.3 kV	6.6 kV	690 V
DC bus voltage	5.6 kV	2.8 kV	5.6 kV	1.05 kV
Grid filter inductance	1.13 mH	1.13mH	2.89mH	0.15 mH
IGCT/IGBT type	5SHY35L4512		5SDF16L4503	FZ3600R17HP4
Diode type	5SHY35L4510		5SDF10H4503	

As an example, a medium-voltage 10 MW full-scale three-level neutral point clamped (3L-NPC) wind power converter using IGCT is demonstrated, the more detailed converter information is included in Tabe I and [52]. The simulation results of junction temperatures for each of the power device in 3L-NPC converter are shown in Fig. 14 (a), where the grid side and generator side converters are indicated respectively under rated and steady-state operation.

It can be seen that for the 3L-NPC wind power converter, the thermal stress of different power devices are quite unequal both on the grid side and on the generator side. On the grid side, the clamping diode Dnpc and outer switch Tout are the hottest devices with much higher junction temperature mean value and fluctuation amplitude compared to other devices - that means shorter life time to failure according to Fig. 12. On the generator side, the freewheeling diodes Dout and Din are becoming the hottest devices.

The envelop of junction temperature excursion for the most stressed devices in 10 MW 3L-NPC wind power converter is shown in Fig. 14 (b), where the whole operation range of the wind speeds are investigated. This temperature profile is essential to estimate the reliability performance of the wind power converter and can be used as a reference for the loading improvements of the power devices.

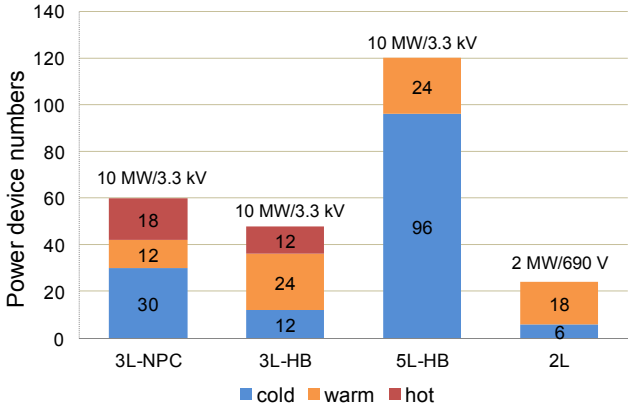

Fig. 16. Device utilization of different converter topologies. (Red color represents the "hot" devices, yellow "warm" devices and blue "cold" devices).

Another example is a low-voltage 2 MW full-scale two-level wind power converter using IGBT, as shown in Fig. 15 (a), where the thermal cycling of grid side and generator side converter are demonstrated respectively. Fig. 15 (b) shows the envelop for the junction temperature excursion of the most stressed devices on the whole operation range of the wind speeds.

It can be seen that different converter topologies may result in different loading and utilization of the power switching devices. According to the mean junction temperature distribution, the power devices in a converter topology can be categorized into three types: the "hot" devices which have mean junction temperature T_{jm} higher than 105 ℃, the "warm" devices which have T_{jm} between 75 ℃ and 105 ℃, and the "cold" devices which have T_{jm} below 75 ℃. The proportion of certain type of power devices will indicate the devices utilization and reliability information of a converter. The numbers of the three types of power devices in different converter topologies are summarized in Fig. 16, in which 3L-

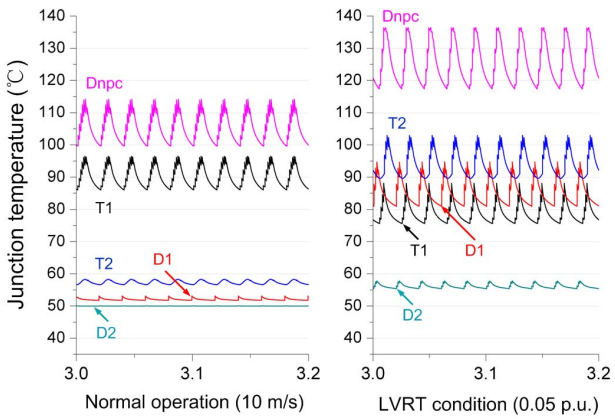

Fig. 17. Thermal distribution of 10 MW 3L-NPC grid inverter. (Normal condition: 6.3 MW output, *PF*=1. LVRT condition: grid voltage 0.05 p.u., providing 100% reactive current) [54].

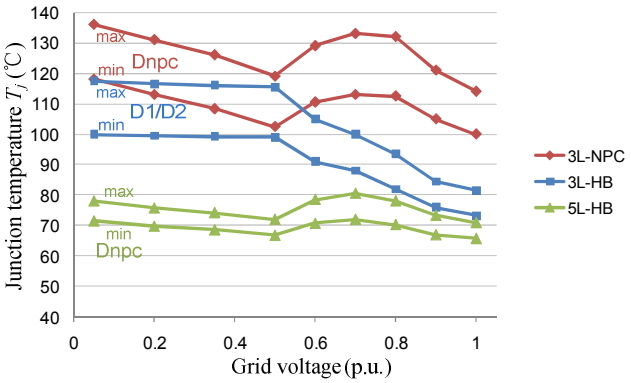

Fig. 18. Junction temperature comparison between 10 MW grid side converter topologies under balanced LVRT (wind speed 10 m/s, most stressed device, reactive current is according to [54]).

NPC, three-level H-bridge 3L-HB, five level H-Bridge 5L-HB [52] and the 2-level converter topologies are illustrated and compared. It can be seen that the 5L-HB, 3L-HB and 2L converter topologies may reduce the numbers of the "hot" devices, achieving more equal and better device loading compared to the 3L-NPC topology.

B. LVRT operation

The grid requirements for the wind turbines especially the low voltage ride through (LVRT) ability during grid faults are getting stricter. It is becoming a trend that the wind turbines should not only withstand the grid faults, but also provide up to 100% reactive current to help the faults recovery [53]. These LVRT requirements may impose large thermal stress to the wind power converter and thus reduce the reliability of the whole generation system.

The junction temperature distribution of 10 MW 3L-NPC converter under three-phase balanced LVRT with 0.05 p.u. grid voltage is shown in Fig. 17 [54]. The thermal distribution under normal operation with 10 m/s wind speed is also illustrated as a reference. It can be seen that the thermal distribution for 3L-NPC is still quite unequal under LVRT operation, and the LVRT operation impose more adverse junction temperature cycling to all of the power switching devices except the outer switch T1.

By using other multilevel converter topologies, the loading profile of power devices during LVRT can be modified. The junction temperature of the most stressed devices in the 3L-NPC, 3L-HB and 5L-HB topologies are compared in Fig. 18, where the junction temperature envelopes are indicated at different grid voltages [54]. It can be seen that the thermal loading under LVRT is quite different with different multilevel topologies. For the 3L-HB topology, it has a better thermal performance compared to the 3L-NPC topology, especially when the grid voltage is above 0.5 p.u.. The 5L-HB shows the best temperature performance among the three topologies. This also means that it has more potential to handle higher power or reduce the cost for cooling system or power semiconductors.

Another way to improve the thermal loading of power device is by modulation. Some thermal optimized modulation methods for the 3L-NPC wind power converter during extreme LVRT are reported in [55]. The basic idea of these modulations is to select the proper vector sequences which can reduce the dwelling time or commutations involving zero voltage level. The loss and thermal in the most stressed devices (clamping diode Dnpc and inner switch Tin) can thereby be reduced. Fig. 19 shows the outputs of a 3L-NPC grid side converter under LVRT with thermal optimized vector sequence, which avoids using the state vector "***111***" (because state vector ***111*** outputs zero voltage level for all of the three phases) and achieves less utilization of Tin and Dnpc.

The dynamic thermal performance of 3L-NPC wind power inverter, which goes from normal operation to extreme

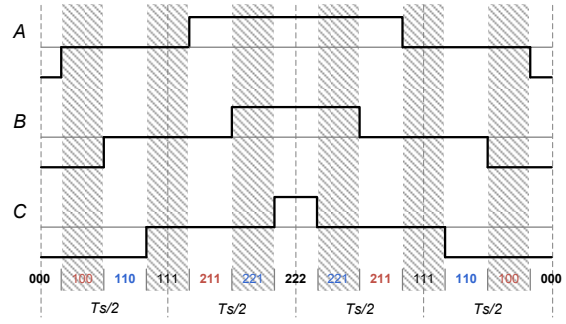

(a) Space vector sequence

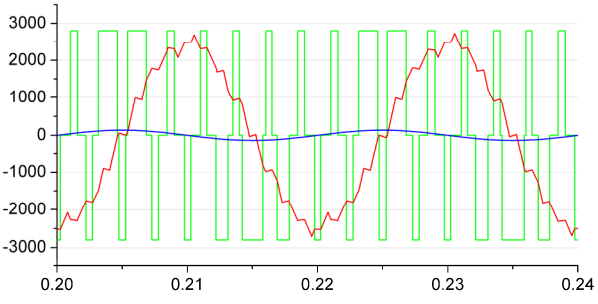

(b) Output voltage pulses (Green), grid voltage (blue), phase current (red). V_g=0.05 p.u

Fig. 19. Thermal optimized modulation sequence for 3L_NPC inverter during LVRT

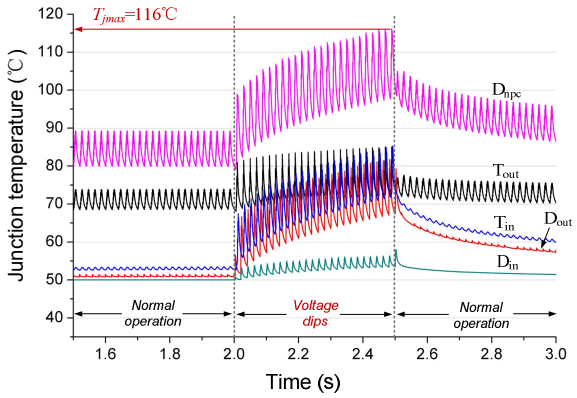

(a) Normal modulation method is applied during LVRT.

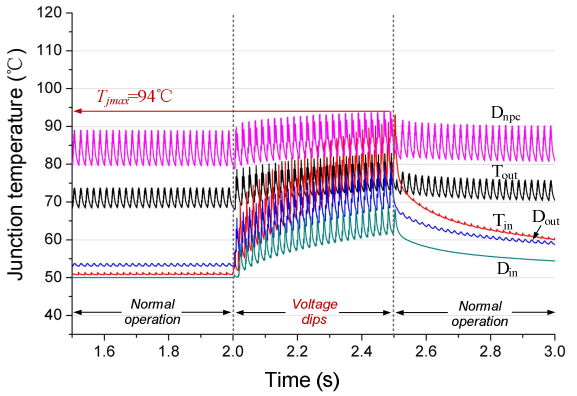

(b) Thermal optimized modulation method is applied during LVRT.

Fig. 20. Dynamic response of junction temperature with a voltage dip time 500 ms (from normal operation with wind speed 8 m/s to 0.05 p.u. LVRT, and then back to normal operation)

LVRT and then back to normal operation, can also be simulated. The junction temperature of each power device when applying different modulation methods during LVRT is shown in Fig. 20. If the optimized modulation method is applied, as shown in Fig. 20 (b), the maximum junction temperature in D_{npc} keeps nearly unchanged and less fluctuated compared to the normal modulation in Fig. 20 (a), and a more equal thermal distribution during LVRT can be achieved.

C. *Wind gust operation*

The thermal cycling with longer time period, which is caused by the load changes, also has strong impacts on the reliability of wind power converter. An example of wind gust is indicated in Fig. 21 (a) where the wind speeds and corresponding current references for the converter are indicated [51]. Fig. 22 (a) shows the junction temperature response of the 10 MW 3L-NPC inverter under the predefined wind gust. It can be seen that as the most stressed device, the clamping diode D_{npc} has up to 43 K junction temperature fluctuation range which may be harmful for the life time of power devices.

As investigated in [51], the reactive power may introduce significantly increased junction temperature to the most stressed devices of 3L-NPC inverter. This feature can be utilized to heat up the power devices in a proper manner so that the fluctuation of junction temperature ΔT_j during load changes can be stabilized. (ΔT_j is claimed be more harmful to the reliability of the power switching devices compared to the average mean junction temperature T_{jm}, as indicated in [46], [56], [57]). Unfortunately, the delivered reactive power to the power grid by the wind power inverters should be limited by grid codes, which normally define a much narrower region for the allowable reactive power than the converter ability. However, for wind power converter systems in a wind farm, the grid side inverters are connected to a local grid, therefore the reactive power can basically be circulated among the inverters locally and not necessarily be seen in the power grid, as shown in Fig. 23. In this condition, the operation range of reactive power is not restrained by the grid codes but by the converter ratings.

Fig. 24 shows one possible current reference generating method, by which the reactive current is adjusted during wind gust to stabilize the mean junction temperature in the most stressed device. In this control system a junction temperature estimation block is important to accurately estimate the average junction temperature of target power devices based on the measured voltages, currents and ambient temperature of the converter.

Fig. 22 (b) shows the thermal cycling performances of devices with the same wind gust operation as Fig. 22 (a) by enabling the thermal control method. It can be seen that junction temperature fluctuation range during the wind gust in D_{npc} reduces from 43K without any reactive power control to 24K with the proposed reliability optimized control. It can be seen that when introducing the reactive power compensation in paralleled converter 2 with overexcited reactive current, the maximum junction temperature of the most stressed devices Dnpc in Fig. 22 (c), is not further more increased.

It is also noted that the reactive power is only circulated inside the parallel converters in order to heat up the power switching devices and is not injected into the power grid. The target of the reactive power control method is different from

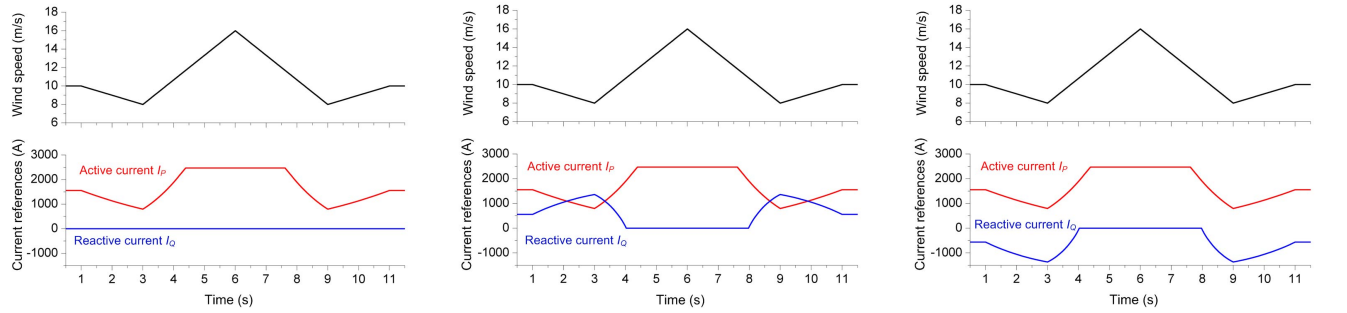

(a) Without reactive power (b) With underexcited reactive power (c) With overexcited reactive power

Fig. 21. Wind gust and current references of 3L-NPC inverter for case study.

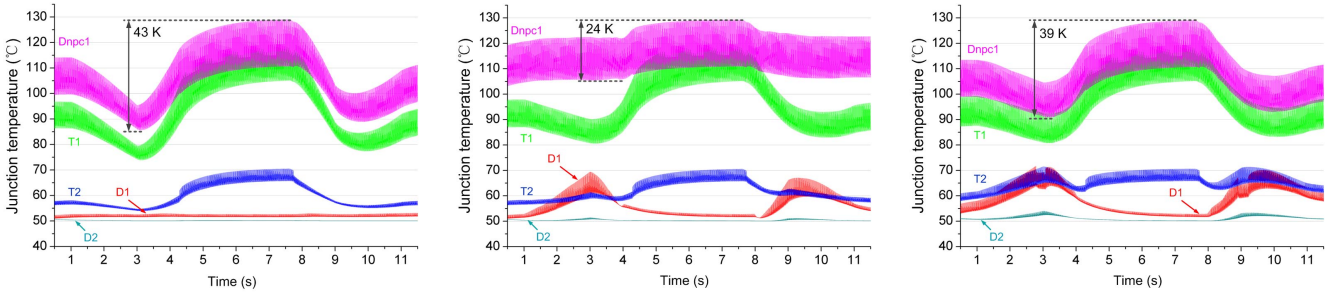

(a) Without reactive power (b) With underexcited reactive power (c) With overexcited reactive power

Fig. 22. Thermal cycling of 3L-NPC inverter during wind gust.

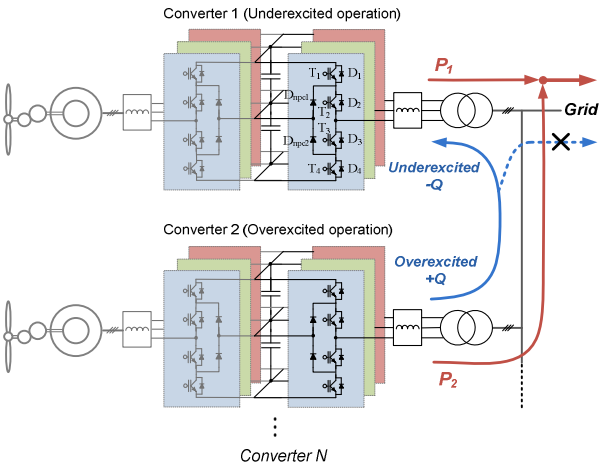

Fig. 23. Reactive power circulated in paralleled wind power converters.

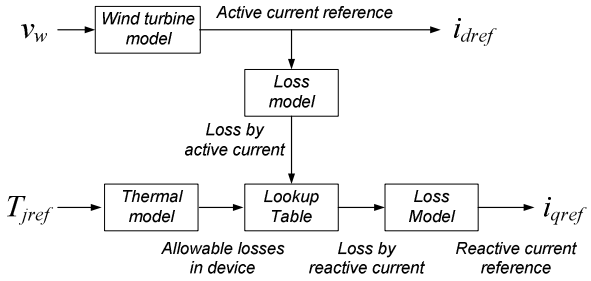

Fig. 24. The basic idea and used models for calculating the active and reactive current references of Fig. 22 (b). (v_w is the wind speed, T_{jref} is the target junction temperature mean value to be stablized in the most stressed devices.)

the regular one used to support the grid voltage. However, the operation modes and reactive power controls of the converter can be switched depending on the grid condition in the real system.

V. Conclusion

As the quick development of technologies and various application requirements for renewable energies, there are many possible power converter configurations as well as circuit topologies in this field. Besides improving the power controllability and performances, more and more efforts are put into making renewable energy systems better in terms of reliability in order to ensure a high availability of the power sources.

In the wind turbines application, the reliability and power controllability are two of the most important performances for the wind power converter. Partial-scale converter systems are now being pushed to full-scale converter systems, where the reliability and cost of power electronics are becoming emerging considerations. While in the photovoltaic application, the efficiency and ground current (for transformer-less configuration) are two of the most important considerations for the PV converters, the single-phase converter topologies are dominant in this field.

The study of reliability in power electronics is moving from a statistically based approach to a physics-of-failure approach, which involves the investigating of the physical failure mechanism and analytical lifetime models of power semiconductors. New ways to evaluate/design the converter system considering the reliability performances can thereby be enabled. Some other potential works on this topic is now being opened: e.g. further understanding and modeling of failure mechanisms, real time detection of the wear-out states of power devices, and thermal-oriented control for power converters, etc.

By modifying the converter topology and using special control or modulation methods, it is possible to improve the thermal loading of wind power converters under various operating conditions, resulting in increased reliability and reduced cost of power semiconductors. It is noted that the thermal loading and the improving effects depend very much on the applications and the selection of power switching devices.

References

[1] S. Heier, "*Grid integration of wind energy conversion systems*", translated by Rachel Waddington, John Wiley, 1998. ISBN-10: 0-47-197143X.

[2] J. M. Guerrero, F. Blaabjerg, T. Zhelev, K. Hemmes, E. Monmasson, S. Jemei, M. P. Comech, R. Granadino, J. I. Frau, "Distributed Generation: Toward a New Energy Paradigm," *IEEE Industrial Electronics Magazine*, vol.4, no.1, pp.52-64, March 2010.

[3] A.D. Hansen, F. Iov, F. Blaabjerg, L.H. Hansen, "Review of contemporary wind turbine concepts and their market penetration", *Journal of Wind Engineering*, 28(3), 2004, pp. 247-263.

[4] Z. Chen, E. Spooner, "Grid Power Quality with Variable-Speed Wind Turbines", *IEEE Trans. on Energy Conversion*, 2001, vol. 16, no.2, pp. 148-154.

[5] M.P. Kazmierkowski, R. Krishnan, F. Blaabjerg,"*Control in Power Electronics-Selected problems*", Academic Press, 2002. ISBN 0-12-402772-5.

[6] R. Pena, J.C. Clare, G.M. Asher, "Doubly fed induction generator using back-to-back PWM converters and its application to variable speed wind-energy generation", *IEE Electric Power Application*, 1996, vol. 143, no.3, pp. 231-241.

[7] K. Wallace, J.A. Oliver, "Variable-Speed Generation Controlled by Passive Elements", Proc. of ICEM, 1998, pp. 1554-1559.

[8] J.B. Ekanayake, L. Holdsworth, W. XueGuang, N. Jenkins, "Dynamic modelling of doubly fed induction generator wind turbines", *IEEE Trans. on Power Systems*, 2003, vol. 18, no. 2, pp. 803-809.

[9] F. Blaabjerg, Z. Chen, S.B. Kjaer, "Power Electronics as Efficient Interface in Dispersed Power Generation Systems", *IEEE Trans. on Power Electronics*, 2004, vol. 19, no. 4, pp. 1184-1194.

[10] L. Mihet-Popa, F. Blaabjerg, I. Boldea, "Wind Turbine Generator Modeling and Simulation Where Rotational Speed is the Controlled Variable", *IEEE Trans. on Industry Applications*, 2004, vol. 40, no. 1. pp. 3-10.

[11] N. Flourentzou, V.G. Agelidis, G.D. Demetriades, "VSC-Based HVDC Power Transmission Systems: An Overview," *IEEE Trans. on Power Electronics*, vol.24, no.3, pp.592-602, March 2009.

[12] Z. Chen, J.M. Guerrero, F. Blaabjerg, "A Review of the State of the Art of Power Electronics for Wind Turbines," *IEEE Trans. on Power Electronics,* vol.24, no.8, pp.1859-1875, Aug. 2009.

[13] T. Shimizu, M. Hirakata, T. Kamezawa, H. Watanabe, "Generation Control Circuit for Photovoltaic Modules", *IEEE Trans. on Power Electronics*, 2001, vol. 16, no. 3, pp. 293-300.

[14] B. Yang; W. Li, Y. Zhao, X. He; , "Design and Analysis of a Grid-Connected Photovoltaic Power System," , *IEEE Trans. on Power Electronics*, vol.25, no.4, pp.992-1000, April 2010.

[15] Y. Sozer, D.A. Torrey, "Modeling and Control of Utility Interactive Inverters," *IEEE Trans. on Power Electronics,* vol.24, no.11, pp.2475-2483, Nov. 2009.

[16] K. Jung-Min, K. Bong-Hwan, N. Kwang-Hee, "Three-Phase Photovoltaic System With Three-Level Boosting MPPT Control," *IEEE Trans. on Power Electronics*, vol.23, no.5, pp.2319-2327, Sept. 2008.

[17] M. Liserre, R. Teodorescu, F. Blaabjerg, "Stability of photovoltaic and wind turbine grid-connected inverters for a large set of grid impedance values," *IEEE Trans. on Power Electronics,* vol.21, no.1, pp. 263- 272, Jan. 2006.

[18] M. Ciobotaru, V. G. Agelidis, R. Teodorescu, F. Blaabjerg, "Accurate and Less-Disturbing Active Anti-islanding Method Based on PLL for Grid-Connected Converters," *IEEE Trans. on Power Electronics*, vol.25, no.6, pp.1576-1584, June 2010.

[19] M. Liserre, F. Blaabjerg, R. Teodorescu, "Grid Impedance Estimation via Excitation of LCL -Filter Resonance," *IEEE Trans. on Industry Applications,* vol.43, no.5, pp.1401-1407, Sept.-oct. 2007.

[20] F. Blaabjerg, M. Liserre, K. Ma, "Power Electronics Converters for Wind Turbine Systems," *IEEE Trans. on Industry Applications,* vol.48, no.2, pp.708-719, Mar-Apr. 2012.

[21] F. Blaabjerg, F. Iov, T. Terekes, R. Teodorescu, K. Ma, "Power electronics - key technology for renewable energy systems," in *Proc. PEDSTC* 2011, pp. 445-466, 2011.

[22] S. Muller, M. Deicke, R.W. De Doncker, "Doubly fed induction generator systems for wind turbines," *IEEE Industry Applications Magazine*, vol.8, no.3, pp.26-33, May/Jun 2002.

[23] D. Xiang, Li Ran, P.J. Tavner, S. Yang, "Control of a doubly fed induction generator in a wind turbine during grid fault ride-through," IEEE Transactions on Energy Conversion, Vol.21, no.3, pp. 652-662, Sept. 2006.

[24] D. Schreiber, "Power converter circuit arrangement for generators with dynamically variable power output", US Patent App. 10/104,474, 2002.

[25] B. Andresen, J. Birk,"A high power density converter system for the Gamesa G10x 4.5 MW Wind turbine", *Proc. of EPE* 2007, pp. 1-7, 2007.

[26] R. Jones, P. Waite, "Optimised power converter for multi-MW direct drive permanent magnet wind turbines," in *Proc. Of EPE* 2011, pp. 1-10, 2011.

[27] S. Kouro, M. Malinowski, K. Gopakumar, J. Pou, L. G. Franquelo, B. Wu, J. Rodriguez, M. A. Perez, J. I. Leon, "Recent Advances and Industrial Applications of Multilevel Converters," *IEEE Trans. on Industrial Electronics*, vol. 57, no. 8, pp. 2553 – 2580, 2010.

[28] R. Teichmann, S. Bernet, "A comparison of three-level converters versus two-level converters for low-voltage drives, traction, and utility applications." *IEEE Trans. on Industry Applications*, vol. 41, no.3, pp. 855-865, 2005.

[29] K. Ma, F. Blaabjerg, "Multilevel Converters for 10 MW Wind Turbines," in *Proc. of EPE* 2011, pp. 1-10, 2011.

[30] T. Bruckner, S. Bernet, H. Guldner, "The active NPC converter and its loss-balancing control," *IEEE Trans. on Industrial Electronics*, vol. 52, no. 3, pp.855-868, 2005.

[31] W. Kleinkauf, G. Cramer, and M. Ibrahim, "PV Systems Technology - State of the art developments and trends in remote electrification," SMA Technologie AG, Dec. 01, 2005.

[32] M. Calais, V. Agelidis, "Multilevel converters for single-phase grid connected photovoltaic systems, an overview," in *Proc. of ISIE*'08, 1998, pp. 224-229.

[33] N. Jenkins, "Photovoltaic systems for small-scale remote power supplies," *Power Engineering Journal*, vol. 9, no. 2, Apr. 1995, pp. 89-96.

[34] M. Svrzek, G. Sterzinger, "Solar PV Development: Location of Economic Activity," Renewable Energy Policy Report 2005.

[35] M. Abella and F. Chenlo, "Choosing the right inverter for grid-connected PV systems," *Renewable Energy World*, vol. 7, no. 2, Mar-Apr. 2004, pp. 132-147.

[36] S. B. Kjaer, J. K. Pedersen, F. Blaabjerg; "A review of single-phase grid connected inverters for photovoltaic modules," *IEEE Trans. on Industry Applications*, vol. 41, no. 5, Sep. 2005, pp. 1292- 1306.

[37] O. Lopez, R. Teodorescu, and J. Doval-Gandoy; "Multilevel transformerless topologies for Single-Phase Grid-Connected Converters", *Proc. of ISIE*, 2006, pp. 5191-5196.

[38] H. Schmidt and C. Siedle, J. Ketterer; "EP 1 369 985 A2", Dec. 10, 2003.

[39] T. Kerekes, R. Teodorescu, M. Liserre, C. Klumpner, M. Sumner, "Evaluation of Three-phase Transformerless Photovoltaic Inverter Topologies," *IEEE Trans. on Power Electronics*, Vol. 24, No. 9, pp. 2202-2211, 2009.

[40] European Commission Climate Action, "The EU climate and energy package", March 2007.

[41] S. Faulstich, P. Lyding, B. Hahn, P. Tavner "Reliability of offshore turbines– identifying the risk by onshore experience," European Offshore Wind Energy Conference 2009, Stockholm.

[42] B. Hahn, M. Durstewitz, K. Rohrig "Reliability of wind turbines – Experience of 15 years with 1500 WTs", Wind Energy: Proceedings of the Euromech Colloquium, S. 329–332, Springer-Verlag, Berlin..

[43] E. Wolfgang, L. Amigues, N. Seliger and G. Lugert, "Building-in Reliability into Power Electronics Systems". The World of Electronic Packaging and System Integration, 2005, pp. 246-252.

[44] D. Hirschmann, D. Tissen, S. Schroder, R.W. De Doncker, "Inverter design for hybrid electrical vehicles considering mission profiles," IEEE Conference on Vehicle Power and Propulsion, 7-9 Sept. 2005, pp. 1-6.

[45] C. Busca, R. Teodorescu, F. Blaabjerg, S. Munk-Nielsen, L. Helle, T. Abeyasekera, P. Rodriguez, "An overview of the reliability prediction related aspects of high power IGBTs in wind power applications," *Microelectronics Reliability*, Vol. 51, no. 9-11, September-November 2011, pp. 1903-1907.

[46] A. Wintrich, U. Nicolai, T. Reimann, "Semikron Application Manual," pp. 128, 2011.

[47] I.F. Kovacevic, U. Drofenik, J.W. Kolar, "New physical model for lifetime estimation of power modules," in *Proc. IPEC'10*, pp. 2106-2114, 2010.

[48] E. E. Kostandyan, J. D.Sørensen, "Reliability Assessment of Solder Joints in Power Electronic Modules by Crack Damage Model for Wind Turbine Applications", *Energies*, 2011, Vol. 4, Issue 12.

[49] J. Due, S. Munk-Nielsen, Rasmus Nielsen, "Lifetime investigation of high power IGBT modules", in *Proc. of EPE* 2011, pp. 1-10.

[50] S. Yang, D. Xiang, A. Bryant, P. Mawby, L. Ran, P. Tavner, "Condition Monitoring for Device Reliability in Power Electronic Converters: A Review," *IEEE Trans. on Power Electronics*, vol.25, no.11, pp.2734-2752, Nov. 2010.

[51] K. Ma, M. Liserre, F. Blaabjerg, "Reactive Power Influence on the Thermal Cycling of Multi-MW Wind Power Inverter", in *Proc. of APEC* 2012, pp.262-269, 2012.

[52] K. Ma, F. Blaabjerg, D. Xu, "Power Devices Loading in Multilevel Converters for 10 MW Wind Turbines," in *Proc. of ISIE* 2011, pp. 340-346, June 2011.

[53] M. Altin, O. Goksu, R. Teodorescu, P. Rodriguez, B. Bak-Jensen, L. Helle, "Overview of recent grid codes for wind power integration," *Proc. of OPTIM* 2010, pp.1152-1160, 2010.

[54] K. Ma, F. Blaabjerg, M. Liserre, "Thermal analysis of multilevel grid side converters for 10 MW wind turbines under Low Voltage Ride Through," in *Proc. of ECCE 2011*, pp. 2117 - 2124, Sep 2011.

[55] K. Ma, F. Blaabjerg, "Thermal Optimized Modulation Methods of Three-level Neutral-Point-Clamped Inverter for 10 MW Wind Turbines under Low Voltage Ride Through," *IET Power Electronics*, 2012 (to appear).

[56] W. Lixiang, J. McGuire,R.A. Lukaszewski, "Analysis of PWM Frequency Control to Improve the Lifetime of PWM Inverter," *IEEE Trans. on Industrial Applications,* vol. 47, no. 2, pp. 922-929, 2011.

[57] N. Kaminski, "Load-Cycle Capability of HiPaks," ABB Application Note 5SYA 2043-01, Sep 2004.